Microbiol Monogr (3)
D. Schüler: Magnetoreception and Magnetosomes in Bacteria
DOI 10.1007/7171_040/Published online: ■ September 2006

Structure, Behavior, Ecology and Diversity of Multicellular Magnetotactic Prokaryotes

Carolina N. Keim[1] · Juliana Lopes Martins[1] · Henrique Lins de Barros[2] · Ulysses Lins[1] · Marcos Farina[3] (✉)

[1]Instituto de Microbiologia Professor Paulo de Góes, Universidade Federal do Rio de Janeiro, Centro de Ciências da Saúde, Bloco I, 21941-590 Rio de Janeiro, Brazil

[2]Centro Brasileiro de Pesquisas Físicas, Rua Xavier Sigaud 150, Urca, 22290-180 Rio de Janeiro, Brazil

[3]Instituto de Ciências Biomédicas, Universidade Federal do Rio de Janeiro, Centro de Ciências da Saúde, Bloco F, sala F2-027, 21941-590 Rio de Janeiro, Brazil
mfarina@anato.ufrj.br

Abstract Multicellular magnetotactic prokaryotes (MMPs) show a spherical morphology and are composed of 15–45 cells organized around an internal acellular compartment. Each cell presents a pyramidal shape with the apex of the pyramid facing this compartment The base, where the flagella are attached, faces the environment. MMPs display either a straight or a helical trajectory, and the sense of rotation of the trajectory (clockwise) is the same as the rotation of the microorganism's body during swimming. This is different to what would be expected if the flagella formed a bundle. The fact that MMPs present non-uniform velocities during "ping-pong movement" or "escape motility" further confirms the need for complex coordination of the action of flagella. The organisms express an unusual life cycle. Each organism grows by enlarging the cell volume, not the cell number; then, the number of cells doubles, the organism elongates, then it becomes eight-shaped, and finally splits into two equal spherical organisms. Most multicellular magnetotactic prokaryotes produce greigite (Fe_3S_4) magnetosomes, whereas recent observations show that these organisms can also biomineralize magnetite (Fe_3O_4). All data available on MMPs indicate that they constitute an important model for studies on multicellularity, biomineralization, and evolution in prokaryotes.

1 Introduction

In 1975 Richard Blakemore reported the astonishing discovery of magnetotactic bacteria (MB). These microorganisms contained chains of nanometer-sized iron-rich crystals and were capable of aligning and migrating along the lines of a magnetic field (Blakemore 1975). It was hypothesized that MB use the interaction with the geomagnetic field to swim to the bottom of marine and freshwater environments, where they could find microenvironments with lower levels of oxygen. This suggestion was strengthened after the finding that bacteria collected in either the northern or southern hemispheres (Frankel et al. 1979; Blakemore et al. 1980; Kirschvink 1980) swim to the bottom, towards the sediments. This behavior was called magnetotaxis (the passive orientation along the lines of a magnetic field, and active migration because of the flagella). Later, Frankel et al. (1997) described the behavior of a marine magnetotactic coccus that used magnetotaxis in conjunction with aerotaxis (magneto-aerotaxis), "to more efficiently migrate to and maintain position at their preferred oxygen concentration".

Several studies characterized the crystalline inclusions and the bacteria that produce them (for a review, see Bazylinski and Frankel, 2004). Initially, crystals were identified as magnetite by different methods and crystal morphologies were shown to be species- or strain-specific by high resolution transmission electron microscopy. However, in 1990, the crystalline inclusions found in multicellular magnetotactic prokaryotes were shown to contain iron sulfides (Farina et al. 1990; Mann et al. 1990). This finding opened new questions about the biomineralization phenomenon in prokaryotes.

TS[a] please confirm running title

Editor's or typesetter's annotations (will be removed before the final TEX run)

2
Similar Microorganisms, Different Designations

In 1983, a spherical, large, south-seeking magnetotactic microorganism was reported in the coastal metropolitan lagoon "Rodrigo de Freitas", in Rio de Janeiro city (Farina et al. 1983). Their crystalline inclusions were not studied in detail at that time and were assumed to contain magnetite. Actually, the authors stated that a fraction of the crystalline inclusions observed by transmission electron microscopy (TEM) were composed of magnetite. The inclusions were estimated to contain about 10% of magnetite (Farina et al. 1983) based on TEM data and calculation of the magnetic moment of a population of microorganisms, obtained from the trajectories under an applied magnetic field of known intensity that was reversed (the U-turn method). Later, the microorganism was called magnetotactic multicellular aggregate (MMA) (Farina et al. 1990). This microorganism was different from the MB previously described, in several aspects. It was larger (5–10 μm in diameter) and composed of several cells enveloped by double membranes (Farina et al. 1983, 1990; Lins de Barros et al. 1990a).

Rodgers et al. found a similar microorganism in marine and brackish coastal sites in New England and called it many-celled magnetotactic prokaryote (Rodgers et al. 1990a) or multicellular magnetotactic prokaryote (Rodgers et al. 1990b), both denominations shortened to MMP. The microorganism presented a "rosette or mulberry-like" morphology, was approximately 12.5 μm in diameter, showed a swimming speed ranging from 67 to 175 $\mu m\, s^{-1}$ and was similar in general morphology to the one described by Farina et al. (1983, 1990). It was argued that its complex motility (never observed when the individual cell components of the MMP were seen separated from the body) implied coordination of flagellar activity, and thus communication between cells of the whole organism. Based on the putative membrane adhesion structure observed and on the microorganism's behavior, the authors proposed that the MMP was in fact a multicellular prokaryote (Rodgers et al. 1990a,b). When exposing MMPs to a 60 Hz AC magnetic field, the microorganisms could be remagnetized (many originally north-seeking MMPs could migrate as south-seeking microorganisms), indicating that the intact organism probably has an axis of motility (Rodgers et al. 1990a,b), similar to unicellular MB (Blakemore 1982).

Keim et al. (2004a) described a morphologically similar microorganism in one of the largest hypersaline lagoons in the world, the Araruama Lagoon in Rio de Janeiro State, Brazil (Fig. 1). Because the designation "magnetotactic multicellular aggregate" or MMA became inadequate after the results shown in the paper, and the designation MMP referred to a 16S rDNA study (DeLong et al. 1996), the denomination magnetotactic multicellular organism (MMO) was proposed for these microorganisms. Here we will use the designation MMP for all of them.

Table 1 Comparison of MMP main characteristics and the environments where they are found

Size (μm)	Cell number	Cell size	Speed (μm/s)	Type of magnetic crystal	Crystal size (nm)	Site of collection	Salinity (‰)	pH	Refs.
5–9	15–25	1.5–2.5 × 1–2 μm	30 and 100	Fe sulfide	75–100	RFL	~ 8*		Farina et al. 1983, 1990; Lins de Barros et al. 1990
2.2–4.6		0.33 ± 0.2 μm^3		Fe sulfide *		RFL	~ 8*		Lins and Farina, 1999
4–12	10–30			Fe sulfide	75 (mean)	SP, WH, NRM, PRWR	12–32		Bazylinski et al. 1990
3–8	7–20			Fe sulfide	75 (mean)	Marine and brakish sites	12–31		Mann et al. 1990
3–12.5	10–30	0.8–1.4 × 0.6–0.8 μm	105 (mean)	Fe sulfide	85–90	NE	12–32	7.3–6.5	Rodgers et al. 1990a
	15–20			Fe sulfide	30–120	SP, PRWR, SSNP	~ 29	~ 7.4	Pósfai et al. 1998a,b
				Fe sulfide	74 ± 18	PRWR, SSNP			Pósfai et al. 2001
						SP	18–28	7–9	Simmons et al. 2004
5.5–9.5	17.4 ± 3.59		90 ± 20	Fe sulfide		Ara	74.55	~ 7.4	Keim et al. 2004a,b; Almeida et al. 2005
			~ 100			WH			Greenberg et al. 2005
4–7				Fe sulfide	45–55	Enc	~ 50		Martins et al. submitted
				Fe oxide+ Fe sulfide		Rob	~ 50	~ 7.0*	Martins et al. submitted
5.3 ± 0.6*				Fe oxide+ Fe sulfide	70 ± 8 104 ± 29	Ita	32–35*	~ 7.0*	Keim et al. 2003; Lins et al. submitted

Table 1 (continued)

Abbreviations:	
Ara	Araruama Lagoon, a large lagoon at the coast of Rio de Janeiro State, Brazil
Enc	Encantada Lagoon, a small coastal lagoon at Restinga de Jurubatiba National Park, Rio de Janeiro State, Brazil
Ita	Itaipu Lagoon, a coastal lagoon in the metropolitan area of Niterói, Rio de Janeiro State, Brazil
NE	Brackish coastal sites on New England coast
NRM	Salt marshes in Neponset River Marsh, Boston, MA, USA
PRWR	Shallow salt-marsh pools in the Parker River Wildlife Refuge, Rowley, MA, USA
RFL	Rodrigo de Freitas Lagoon, a coastal lagoon in Rio de Janeiro city, Brazil
Rob	Robalo Lagoon, a coastal lagoo at Restinga de Jurubatiba National Park, RJ, Brazil
SP	Salt Pond, Woods Hole, MA, USA
SSNP	Sweet Springs Nature Preserve, Morro Bay, CA, USA
WH	Salt marshes in Woods Hole, MA, USA
WNB	Salt marsh pond near Wood Neck beach in Woods Hole, MA
*	Personal observation

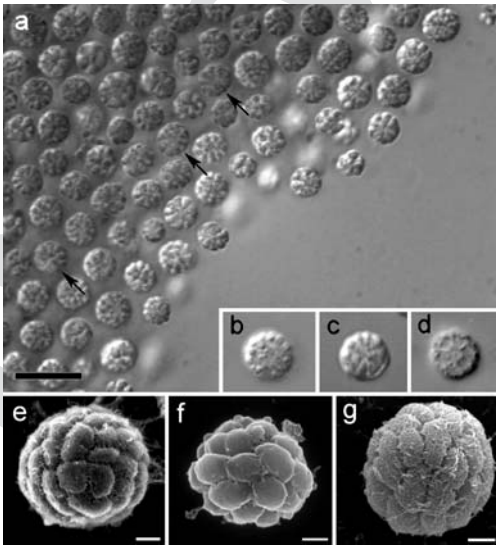

Fig. 1 Diferential interference contrast light microscopy (DIC) and scanning electron microscopy (SEM) of MMPs from: Araruama (**a**), Robalo (**b**), Rodrigo de Freitas (**c**), and Itaipu (**d**) Lagoons (DIC); and Araruama (**e**), Rodrigo de Freitas (**f**), and Encantada (**g**) Lagoons (SEM). *Scale bar* in (**a**) corresponds to 15 μm for (**a**) and 10 μm for (**b**), (**c**), and (**d**). *White bars* = 1 μm for (**e**), 1.5 μm for (**f**), and 3 μm for (**g**). Note the morphological similarity and the spherical shape of the microorganisms. The lack of flagella in (**h**) is due to the sample preparation procedure. The images in (**a**) and (**e**) are reprinted from Keim et al. 2004a with permission from Elsevier

All MMPs seem to share main particularities such as: $\sim 3–12\ \mu m$ in diameter (Farina et al. 1983, 1990; Bazylinski et al. 1990; Lins de Barros et al. 1990a; Mann et al. 1990; Rodgers et al. 1990a,b; Lins and Farina 1999; Keim et al. 2004a,b, Table 1), the fact that they contain several prokaryotic cells apparently organized in a helical symmetry (Farina et al. 1983, 1990; Lins de Barros et al. 1990a; Lins and Farina 1999; Keim et al. 2004b) with all cells facing both the environment and an internal acellular compartment (Keim et al. 2004a), the cells present a glycocalix (Farina et al. 1983; Keim et al. 2004a), several flagella facing the environment (Keim et al. 2004a; Rodgers et al. 1990a), the individual cells are never motile when separated from the whole microorganism (Farina et al. 1990; Lins and Farina 1999; Keim et al. 2004a), and the organism probably has an unique life cycle (Keim et al. 2004b).

These microorganisms have not been cultured until now, and thus all studies were done with samples collected directly from the environment.

2.1 Phylogenetic Studies

Few studies exist on the phylogenetic affiliation of MMPs. The 16S rDNA of MMPs, collected in coastal sites in New England (USA), were sequenced and found to be related to the sulfate-reducing bacteria group within the δ-Proteobacteria, *Desulfosarcina variabilis* being the most closely related cultivated organism found in the databases (DeLong et al. 1993). The 16S rDNA of two different samples collected in 1990 and 1991 showed more than 99% similarity, leading to the conclusion that MMPs comprised a single species (Bazylinski et al. 1993). Recently, part of the 16S rDNA gene of MMPs from Araruama Lagoon was sequenced and presented 87% similarity with the same region of the 16S rDNA gene of MMP 1991 (Keim et al. 2004b), one of the two sequences obtained by DeLong et al. (1993). Several δ-Proteobacteria sequences were identified in a MMP-rich sample, but no sequences identical to previously sequenced MMP clones were found (GenBank accession numbers AY589482, AY589485, and AY589481) (Simmons et al. 2004). All these preliminary results suggest that MMP from the hypersaline Araruama Lagoon may represent a different species, but further work is necessary to evaluate de phylogenetic diversity within the group.

3 Ecology of the Multicellular Magnetotactic Prokaryotes

MMPs have been observed in different regions around the globe (Bazylinski et al. 1990, 1993; DeLong et al. 1993; Farina et al. 1983, 1990; Flies et al. 2005; Greenberg et al. 2005; Keim et al. 2003, 2004a,b; Lins de Barros et al. 1990a; Lins and Farina 1999, 2001; Lins et al. 1992, 2000, submitted; Mar-

tins et al. submitted; Penninga et al. 1995; Pósfai et al. 1998a,b; Rodgers et al. 1990a,b; Simmons et al. 2004, 2006; Winklhofer et al. 2005). Table1 summarizes different characteristics of these microorganisms including the type of magnetic mineral precipitated in their magnetosomes. They occur in anaerobic, brackish to hypersaline, sulfide-rich environments (Bazylinski et al. 1990; Farina et al. 1990; Lins de Barros et al. 1990a; Rodgers et al. 1990a,b; Pósfai et al. 1998b; Lins and Farina, 1999; Keim et al. 2004a; Simmons et al. 2004), in the water column of stratified lagoons (Bazylinski et al. 1990; Rodgers et al. 1990a,b; Pósfai et al. 1998b; Simmons et al. 2004) or in the sediment of aquatic environments with non-stratified water columns (Farina et al. 1990; Lins de Barros et al. 1990a,b; Keim et al. 2004a).

Each type of magnetotactic bacterium seems to be adapted to different chemical and physical gradients in the stratified microenvironments where they thrive (Simmons et al. 2004). Greigite-producing magnetotactic bacteria (including the MMP) are found in the anaerobic zone, just below the oxic–anoxic transition zone (Bazylinski et al. 1995; Pósfai et al. 1998b), whereas unicellular magnetite-producing magnetotactic bacteria are usually found at the oxycline (Simmons et al. 2004).

Simmons et al. (2004) reported results of studies on the distribution of different magnetotactic bacteria with respect to the physical and chemical condition of the environment, at Salt Pond (Falmouth, Massachussetts, USA). They studied the water column (between June and August, 2002) and found that the magnetite-producing bacteria were most abundant at the top of the oxycline, whereas MMP occurred at the bottom of the oxycline, or slightly below it, in regions of low sulfide. In this environment, the MMPs were spatially separated from the magnetotactic cocci.

Because MMPs were found in a relatively narrow window in the chemocline, below the oxycline and at relatively low sulfide concentrations, and the fact that an order of magnitude shift in their population was found within 15 cm, suggest that the MMP is a gradient microorganism, but that its location in the chemical gradient is not directed by the oxygen concentration. Instead, they could be chemotactic to iron or a sulfur compound, since Fe(III) concentrations peaked at the depth where most MMPs were found (Simmons et al. 2004).

3.1
Distribution of MMPs in Coastal Lagoons of Rio de Janeiro

We have been studying the presence of MMPs in several coastal lagoons near Rio de Janeiro city, located in the South Atlantic Geomagnetic Anomaly (low field intensity of about 0.23 Gauss). The geomagnetic field points up with a typical inclination angle of about 25°.

Araruama Lagoon (22°50′21″S, 42°13′44″W) is the largest hypersaline coastal lagoon in Rio de Janeiro State (Kjerfve et al. 1996). Encantada La-

goon is a small coastal lagoon located at the Restinga de Jurubatiba National Park (22° – 22°30′S and 41°15′ – 42°W). Both lagoons are hypersaline environments, with salinity around 50‰, but have a great diversity in water physico-chemical characteristics (Kjerfve et al. 1996; EnrichPrast et al. 2003). We have also been studying MB from Itaipu Lagoon, a brackish coastal lagoon located in Niterói, north-east of Rio de Janeiro, Brazil. Table 1 shows some characteristics of these environments.

MMPs can be obtained from samples of water and sediment after magnetic concentration, as described by Lins et al. (2003). Briefly, samples are put in a special chamber and exposed to a properly aligned magnetic field using a home-made coil connected to a DC power supply that aligns bacteria to swim towards a capillary end, from where the microorganisms are collected.

The only magnetotactic microorganisms found at Araruama Lagoon were MMPs (Fig. 1). We investigated the distribution of MMPs in microcosms consisting of Araruama Lagoon sediment and water stored in 10 L containers. MMPs were directly counted under the microscope after magnetic exposure of a fixed volume of sediment. MMPs were detectable even 42 days after sampling. Monitoring five microcosms, we observed different density population behaviors: the rate that MMP population decreased was variable, and in some cases their number increased (Fig. 2a). This occurs probably because of the biotic and abiotic variations among the microcosms.

To analyze the vertical distribution of MMPs within the microcosms, the top (1 cm) layer of the sediment was repeatedly removed (up to 5 cm) from

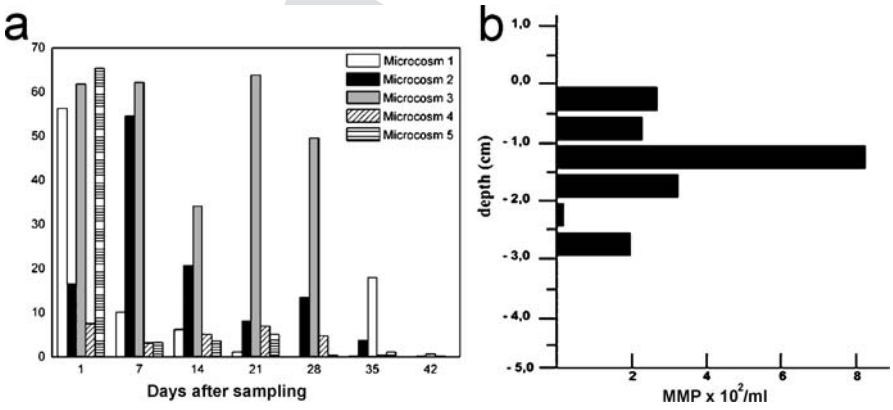

Fig. 2 Distribution of MMPs in microcosms consisting of Araruama Lagoon sediment and water stored in 10 L containers. **a** Number of MMPs in five different microcosms with time, evaluated from small core samples. **b** Distribution of MMPs in sediment cores from microcosms after two weeks. The *bars* show the concentration of MMPs at different depths in the same microcosm, as number of MMPs/mL of sediment. The *scale bar* represents 5 μm

a sample core, immediately diluted with sterile lagoon water, and placed onto a microscope slide. The slide was exposed to the magnetic field of an ordinary magnet for 5 min, when the MMPs that reached the edge of the drop were directly counted with a phase contrast microscope. Figure 2b shows that the MMPs were located up to 3 cm deep in the sediment. In the lagoon, we have observed that the MMPs are found mainly at 3–4 cm deep, and the dissolved oxygen penetration into the sediment does not reach deeper than 0.3 cm (J. L. Martins and U. Lins, unpublished observation).

In sample cores collected around the lagoon in a single day, no MMPs were observed at Rio das Moças estuary, where the salinity was 23.7 ppt, the lowest observed in the samples (Fig. 3). Large populations of MMPs are found at Baleia, Iguabinha and Rebolo beaches, with salinities of 56, 60, and 54.6‰, respectively (Fig. 3). This pattern suggests that the MMPs of Araruama Lagoon occur only in hypersaline conditions (J. L. Martins and U. Lins, unpublished observations).

Denaturing gel gradient electrophoresis (DGGE) profiles of a 16S rDNA fragment showed only one band in all samples of MMPs analyzed (Fig. 4), strongly indicating that genetically identical cells form the MMPs from Araruama and Encantada Lagoons. Further, the same melting behavior observed for the 16S rDNA fragment obtained from MMPs collected at Encantada and Araruama Lagoons (Fig. 4) indicates that these lagoons probably contain the same organism (J. L. Martins and U. Lins, unpublished observations).

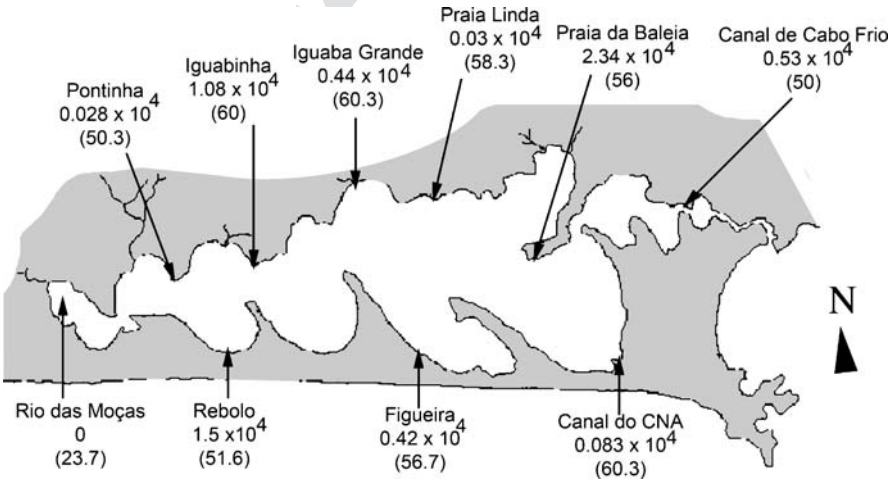

Fig. 3 Distribution of MMPs around Araruama Lagoon in the first 5 cm of sediment, as evaluated from core samples the day after collection. The numbers without parenthesis are the MMP number/mL. The numbers between parenthesis are the salinity (‰) evaluated with a manual refractometer. The city of Rio de Janeiro is located about 50 Km west of this region in the map

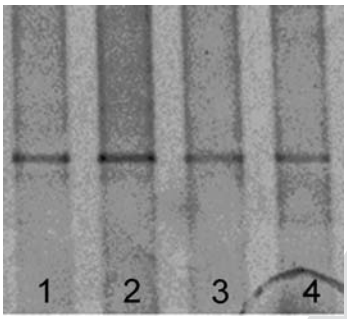

Fig. 4 DGGE profile of a 16S rRNA fragment from magnetically concentrated samples from Encantada (samples 1 and 2) and Araruama (samples 3 and 4) Lagoons. The *single band* in all lanes is indicative of the genetic similarity within and between the samples

4
Morphology of Multicellular Magnetotactic Prokaryotes

MMPs are spherical organisms composed of several cells arranged in a roughly helical disposition (Fig. 1e) (Farina et al. 1983, 1990; Lins de Barros et al. 1990a; Lins and Farina 1999; Keim et al. 2004a). The cells are arranged radially around an acellular internal compartment found at the center of the organism (Figs. 5 and 6) (Keim et al. 2004a,b). The radial arrangement of the cells around the internal compartment causes the cells to assume a pyrami-

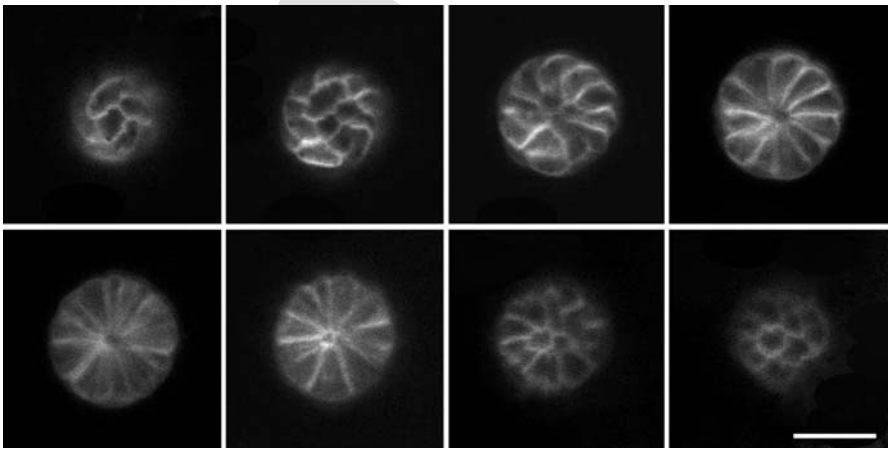

Fig. 5 Confocal laser scanning microscopy (Zeiss 510-META) series of a MMP stained with the lipophylic dye (FM 1-43) that outlines the cell contours; Note that cells are highly elongated radially, with the pointed end in contact with the internal compartment. The *scale bar* represents 5 μm

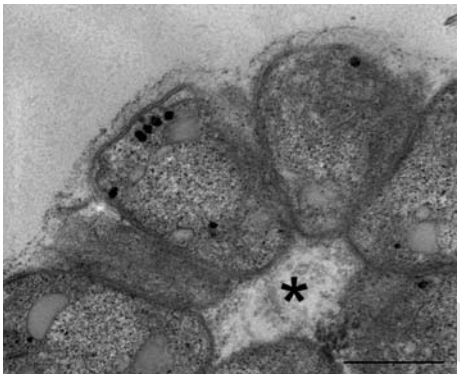

Fig. 6 Ultra-thin section of part of a MMP from Rodrigo de Freitas Lagoon. Note the magnetosomes (*dark regions*), the capsule composed of radial fibers at the organism surface, the lipid droplets (*large inclusions*) and the internal compartment (*asterisk*). The *scale bar* represents 1 μm

dal shape with the bases of the pyramids forming the outer surface of the organism and the apexes lining the internal compartment (Fig. 7a). This compartment contains small membrane vesicles and filaments linking the apex of the pyramids. The pyramid faces are present where the cell is in contact with a neighbor cell, and the edges are present where the cell is in contact with two or more cells (Fig. 7). Accordingly, the pyramid base, which is the part of the cell that faces the environment, is rounded (Fig. 7) (Keim et al. 2004a).

When soap bubbles aggregate to cover space, after a certain number of bubbles, the addition of a new sphere leads to a configuration where one bubble is completely surrounded by others (Williams 1979). Thus we would expect to observe internal cells in the MMPs if only stability of the whole structure, caused by the reduction in surface tension, is considered. In MMPs, specific structures must bind the cells together in specific regions, causing tensions that lead the cells to be elongated in the direction of the center of the organism. Although the internal compartment seems to be a consequence of the organism's architecture, as evidenced by the absence of internal cells and the high level of symmetry of the cells within the microorganisms, it contains fibers that could be involved in binding cells together, and also vesicles that could be involved in cell-to-cell communication. Both functions are supported by the fact that all cells have contact with the internal compartment. Besides, this compartment could be used in cell-to-cell communication through diffusion of soluble molecules. An obvious advantage for an organism having no internal cells is that all cells are in contact with the outside environment, where they take nutrients (Keim et al. 2004a).

MMPs collected in Rodrigo de Freitas Lagoon (Farina et al. 1983, 1990; Lins de Barros et al. 1990a; Lins and Farina, 1999), Itaipu Lagoon (Lins et al. submitted) and Encantada Lagoon (Martins et al. submitted) show the same

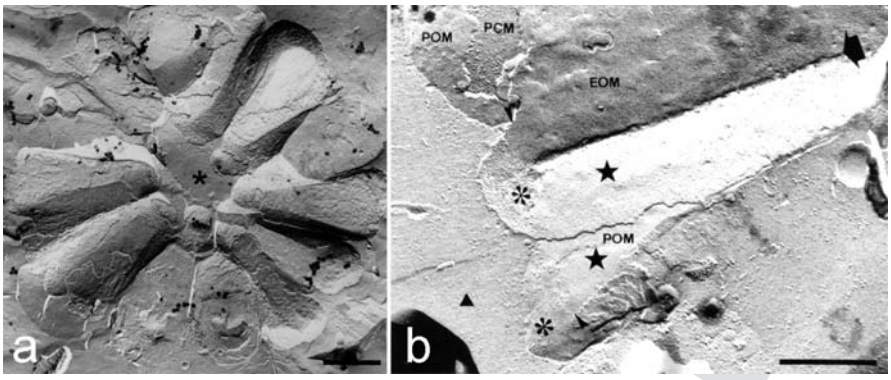

Fig. 7 Freeze-fracture images of MMPs from Araruama Lagoon. **a** The radial arrangement of the cells, the flat membrane surfaces, and the radial edges give the cells a pyramidal shape. The acellular internal compartment fills the central region of the organism (*asterisk*). **b** There are flat membrane surfaces in the region of contact between two cells and a straight groove (*arrow*) in the E-face of the outer membrane (EOM) in the contact region between three cells. Note that the rounded regions, which have direct contact with the environment, present a high concentration of intramembrane particles in both the E-face (*EOM*) and the P-face (*POM*) of the outer membrane (*asterisks*) in comparison with the region of contact between two cells (*stars*). The *triangle* marks the outer environment. The *scale bar* represents 1 μm for (**a**) and 0.5 μm for (**b**). Reproduced from Keim et al., 2004a with permission from Elsevier

general cell organization as those collected in Araruama Lagoon, with the cells arranged around the internal compartment (Fig. 1). MMPs from Rodrigo de Freitas Lagoon frequently exhibits a more evident helical cell arrangement (Farina et al. 1983; Lins de Barros et al. 1990; Lins et al. 1992; Lins and Farina, 1999), in comparison with those from Araruama (Keim et al. 2004a,b) and Encantada, (Martins et al. submitted) Lagoons.

Electron micrographs published on the MMPs from the northern hemisphere (Rodgers et al. 1990a,b) do not enable such comparisons. However, based on the genetic similarity (Keim et al. 2004b), the similarity of the light micrographs (Rodgers et al. 1990a,b; DeLong et al. 1993; Greenberg et al. 2005; Simmons et al. 2004, 2006), and whole mount TEMs (Mann et al. 1990; Bazylinski et al. 1993; Penninga et al. 1995; Pósfai et al. 1998a,b; Simmons et al. 2004), we propose that the cell arrangement described by Keim et al. (2004a), summarized in this section, also corresponds to the cell arrangement of the MMPs from the northern hemisphere.

4.1 The Cell Envelope

The cell envelope presents the double membrane characteristic of gram-negative bacteria (Fig. 6) (Farina et al. 1983, 1990; Lins de Barros et al. 1990a;

Rodgers et al. 1990a; Lins and Farina 2001; Keim et al. 2004a). Between the cytoplasmic and outer membranes (in the periplasmic space), a thin peptidoglycan layer is sometimes seen (Rodgers et al. 1990a; Keim et al. 2004a). The four membranes of adjacent cells are tightly apposed, which indicates the existence of structures specialized to bind cells together (Keim et al. 2004a). The observation of a constant distance of about 2 nm between the outer membranes of adjacent cells led to the proposition that cell junctions could be present in these membranes (Rodgers et al. 1990a). Observation of partially disaggregated MMPs by scanning electron microscopy (SEM) (Lins and Farina 1999) and of whole mounts by TEM (Lins et al. 2000) showed regions of focal contact between adjacent cells. No relationships could be found between the constant distance between the outer membranes (Rodgers et al. 1990a, Keim et al. 2004a) and these regions (Lins and Farina 1999, Lins et al. 2000). Furthermore, freeze fracture results did not show any structures that could be definitely responsible for the focal contacts and for the constant distance observed between the outer membranes (e.g., Fig. 7b). On the other hand, the fact that the outline of the underlying cell could be observed in the E-face (inner face of the external leaflet) of the outer membrane shows that some membrane specialization is present, especially between the region of contact with another cell and the region of contact with the environment (Keim et al. 2004a).

The membrane surfaces of MMP cells are different in each cell region as a result of polarization and specialization of the diverse membrane regions. The surface of the pyramid base, which is the part of the cell in contact with the outer environment, presents flagella (Rodgers et al. 1990a,b; Keim et al. 2004a) which are 21.5 nm in diameter (Rodgers et al. 1990a,b) and a capsule formed by radial fibers (Fig. 6) (Farina et al. 1983; Keim et al. 2004a), probably composed of polysaccharides, 94 ± 18 nm thick (Keim et al. 2004a).

Freeze-fracture replicas of MMPs show mainly outer membrane fracture surfaces (Fig. 7). Cell membrane fracture surfaces appear mainly in the central region of the MMPs (Fig. 7a), suggesting a difference in composition of the cell membrane or the outer membrane at these regions. The replicas of the E-face of the outer membrane show a gradient of intramembrane particles growing toward the center of the organism in the part of the cell that has contact with another cell (Fig. 7b). In the P-face (inner face of the protoplasmic leaflet) of the outer membrane, the part of the cell in contact with the environment shows a higher concentration of intramembrane particles than the part of the cell in contact with another cell. The edges or projections (present where the cell is in contact with two or more cells) also present a higher concentration of intramembrane particles, which is continuous with the part of the cell in contact with the environment. In the part of the outer membrane that faces the environment, there is a high concentration of intramembrane particles in both faces (Fig. 7b), possibly related to metabolic exchange. The boundary between the part of the cell in contact with another cell and the part

of the cell that faces the environment is evident and continuous in adjacent cells (Fig. 7b) (Keim et al. 2004a). The membrane specializations evidenced by the different distribution of intramembrane particles, capsule fibers, and flagella show that the MMP cells are polarized.

4.2 The Cytoplasm

The cells present a cytoplasm rich in ribosomes (Fig. 6) and sometimes a visible nucleoid (Rodgers et al. 1990a). Crystalline organic structures, as well as a structure similar to polar membranes, are present in the cytoplasm (Farina et al. 1983). The structure similar to polar membranes can also be observed in the organisms collected in another place (Keim et al. 2004a,b). Despite the morphological similarity to polar membranes, the fact that these structures are found in the cytoplasm and not associated with the membranes suggests that they are not polar membranes, but structures unique to MMPs.

Large lipid (Keim et al. 2004a) and/or polyhydroxyalkanoate inclusions (Rodgers et al. 1990b, Keim et al. 2004a) are found in the cytoplasm (Fig. 6). They can be distinguished by their characteristic freeze-fracture patterns and by light microscopy after differential staining. MMPs contain large lipid droplets and, sometimes, small polyhydroxyalkanoate inclusions. Polyphosphate bodies containing mainly P, O, and Mg are sometimes found (Keim, unpublished results).

4.3 Organization of the Magnetosomes

The number of iron sulfide magnetosomes in MMPs was reported to vary from 300 (Lins et al. 1992) to about 1000 (Farina et al. 1983, 1990; Lins de Barros et al. 1990a). Some authors reported that the magnetosomes are uniformly distributed between the cells (Pósfai et al. 1998b), whereas others observed a non-homogeneous magnetosome distribution between the cells (Lins de Barros et al. 1990a). Rodgers et al. (1990a) observed that each individual cell presents 2–65 (average 31) magnetosomes. The size of the magnetosome crystals from MMPs are listed in Table 1. In contrast to the magnetite magnetosomes from unicellular bacteria (Devouard et al. 1998), the size distribution of the iron sulfide crystals from the MMPs show an almost perfect Gaussian curve (Pósfai et al. 2001). Magnetosomes are arranged in planar groups in the cytoplasm (Farina et al. 1983; Lins de Barros et al. 1990a; Lins and Farina 1999; Lins et al. submitted) near the periphery of the microorganism, parallel to the surface (Silva et al. 2003; Keim et al. 2004a; Lins et al. submitted). It means that each magnetosome plate is at the largest possible distance from the plates of adjacent cells, considering the spherical symmetry (Silva et al. 2003). Sometimes, the magnetosome chains appear aligned in a whole

MMP (Lins et al. 2000; Penninga et al. 1995; Pósfai et al. 1998b). Whether this alignment reflects the in vivo magnetosome arrangement, or is an artifact caused by the magnetic field used to concentrate the bacteria, remains unknown. A structure resembling a magnetosome membrane of unknown nature is sometimes observed coating the iron sulfide crystals (Farina et al. 1983; Lins de Barros et al. 1990a; Mann et al. 1990).

4.4 Iron Minerals

Crystals in the magnetosomes of MMPs usually have irregular equidimensional shapes (Fig. 6) and are composed of iron sulfides (Farina et al. 1990; Mann et al. 1990; Pósfai et al. 1998a,b; Keim et al. 2004a). High resolution TEM images showed that the iron sulfide crystals were crystallographic single domains (Bazylinski et al. 1990; Mann et al. 1990) with irregular surfaces (Bazylinski et al. 1990). Although most crystals were irregular, some of them show roughly cuboidal, parallelepipedal (Bazylinski et al. 1990, 1993), flake (Bazylinski et al. 1990; Lins de Barros et al. 1990a), "barrel" or bullet shapes (Pósfai et al. 1998b). The iron sulfide magnetosomes from MMPs showed substantial amounts of copper, depending on where they were collected (Bazylinski et al. 1993; Pósfai et al. 1998b). Semi-quantitative energy-dispersive X-ray analysis showed that the crystals are composed of 46–61 atom% sulfur, 37–50 atom% iron and up to 10 atom% copper (Pósfai et al. 1998b).

Iron sulfides in MMPs were first described by Farina et al. (1990) and Mann et al. (1990). Pósfai et al. (1998a,b) performed a detailed crystallographic study with high resolution TEM and electron diffraction and found that MMPs contained the ferrimagnetic greigite (Fe_3S_4), previously reported by Mann et al. (1990) as the magnetic phase, together with non-magnetic mackinawite (tetragonal FeS) and cubic FeS. Greigite was reported as the major phase, followed by mackinawite (Pósfai et al. 1998b), in contrast to an earlier report that described greigite as a minor phase (Mann et al. 1990). Mackinawite was found only at the ends of the magnetosome chains (Pósfai et al. 1998b).

Elemental maps obtained by energy filtering electron microscopy showed that crystals from MMPs presented a peripheral region rich in iron and oxygen (Farina et al. 1990; Lins and Farina 2001; Buseck et al. 2003). The non-magnetic phases, mackinawite and cubic FeS, were proposed to be precursor phases of greigite. It was suggested that cubic FeS would be mineralized, converted to mackinawite and then to greigite through solid-state transformations. These transformations would occur by changes in the position of the iron atoms, with the maintenance of the general structure of the sulfur framework. To transform mackinawite (FeS) into greigite (Fe_3S_4), part of the iron must leave the crystalline lattice (due to stoichiometric relations) (Pósfai et al. 1998a). This surplus iron would account for the amorphous or weakly

crystalline iron-oxygen mineral observed at the periphery where it can be oxidized (Buseck et al. 2003; Farina et al. 1990; Lins and Farina 2001; Lins de Barros et al. 1990a). The crystalline center has a higher iron concentration, a triangular or cuboidal outline, and is 40–45 nm in diameter, whereas the amorphous halo has a lower iron concentration and is 20–25 nm in width (Rodgers et al. 1990a). The crystallographic analysis performed by Pósfai et al. (1998b, 2001) found regions of non-uniform diffraction contrast in iron sulfide crystals; these regions could result from thickness variations or crystalline defects. Iron-oxygen amorphous minerals, 50–70 nm in diameter, were also found in the cytoplasm, and suggested to be iron storage materials (Lins and Farina 2001).

The fact that diamagnetic mackinawite and paramagnetic cubic FeS were found arranged in chains shows that the crystals are aligned in chains before they acquire a permanent dipole moment. Greigite crystals are preferentially aligned with the [100] direction parallel to the chain (the probable easy axis of magnetization in greigite), and thus the biomineralization of the precursor iron sulfide crystals involves a biochemical machinery to mineralize the crystals in the right position in the cell, independently of the magnetic field of the neighboring crystals (Pósfai et al. 1998b). A similar mechanism was recently proposed for magnetite mineralization in *Magnetospirillum* sp. AMB-1 (Komeili et al. 2004).

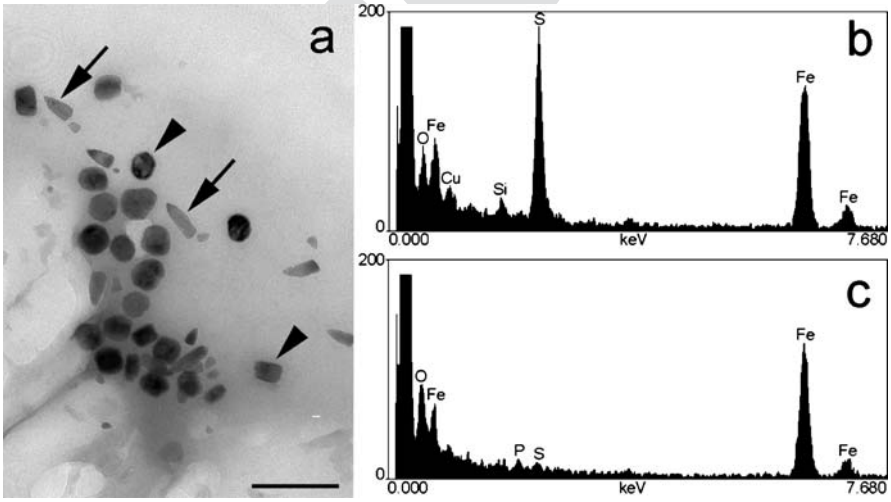

Fig. 8 Observation and elemental analysis of whole mount of a disrupted MMP from Itaipu Lagoon. **a** High magnification of a group of crystals with bullet-shaped (*arrows*) and equidimensional (*arrowheads*) morphologies. The *scale bar* represents 200 nm. **b** Energy-dispersive X-ray (EDX) spectrum of an equidimensional crystal showing iron and sulfur peaks. **c** EDX spectrum of a bullet-shaped crystal showing iron and oxygen peaks. Small P and S peaks are generated by organic constituents of cells

Rarely, magnetite is found in bullet-shaped magnetosomes of MMPs (Keim et al. 2003; Lins et al. submitted), as shown in Fig. 8, and sometimes multiple twins occur (Lins et al. 2000). Bullet-shaped magnetite crystals from MMPs from Itaipu Lagoon are 104 ± 29 nm in length and 42 ± 6 nm in width and are elongated along the [100] direction. Magnetite magnetosomes in MMPs occur alone or together with iron sulfide crystals. MMPs containing only iron sulfides are sometimes found in the same environments as the magnetite-producing MMPs (Lins et al. submitted). Whether magnetite-producing, greigite-producing, and magnetite-greigite-producing MMPs are the same, remains to be discovered. The fact that both types of crystal are found in the same chains suggests that the mechanism of chain assembly is independent of the type of mineral, as suggested for a unicellular magnetotactic bacterium by Bazylinski et al. (1995).

5 Life Cycle

The inheritance of both the magnetic polarity and the movement axis in unicellular MB is epigenetic (Blakemore 1982; Lumsden, 1984; Lins de Barros et al. 1990b; Spring et al. 1998). Considering that the same is occurring in MMPs, which have a more complex body architecture, a complex life cycle is necessary in order to maintain the cell arrangement, the axis of movement, and the magnetic polarity over several generations.

The life cycle of most prokaryotic and eukaryotic multicellular organisms present at least one single-cell stage, i.e., the whole organism can be constructed from a single cell. However, free-swimming individual cells similar to the MMP cells were never observed (Farina et al. 1990; Keim et al. 2004a; Lins and Farina 1999). At least in one environment, MMPs were the only magnetotactic microorganisms found (Keim et al. 2004a,b), excluding the possibility that a small number of magnetotactic unicellular MMP cells could be present in the samples and mistaken for different bacteria. Furthermore, disaggregation in adverse conditions, such as high and low osmolarity, led to a loss of motility (Farina et al. 1990; Lins and Farina, 1999; Lins de Barros et al. 1990a; Mann et al. 1990; Rodgers et al. 1990) and magnetic orientation (Farina et al. 1990). Restoration to the original osmolarity does not restore the motility (Lins de Barros et al. 1990a). Thus, there are no known unicellular stages in the MMP life cycle.

Although most MMPs present a spherical shape, elliptical (Martins et al. submitted; Rodgers et al. 1990) and eight-shaped (Lins and Farina 1999; Martins et al. submitted) organisms are sometimes observed. In fact, these unusual shapes would represent stages of the life cycle of these organisms, as illustrated in Fig. 9. According to this life cycle, MMPs would be spherical for most of their lifetime and would increase in size by increasing the cell

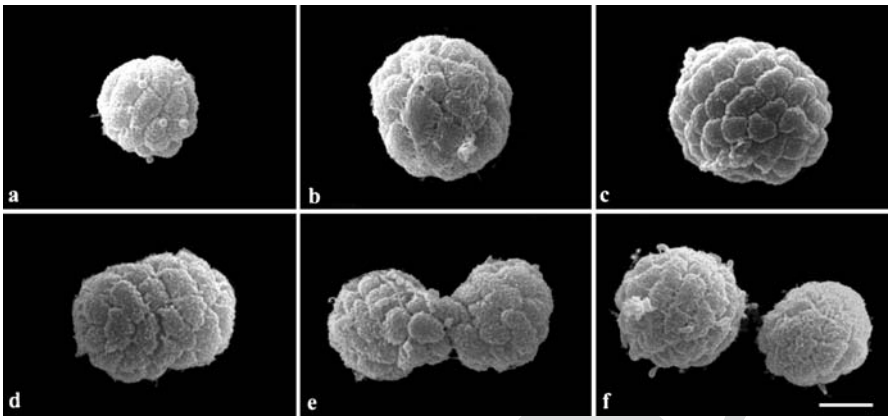

Fig. 9 Sequence of SEM images illustrating the life cycle proposed for MMPs. The MMP is small (**a**) and grows by increasing the cell volume, not the cell number (**b**). Then its cells divide synchronously producing a MMP with twice the cell number (**c**). The organism elongates (**d**) and a constriction appears at the middle (**e**). Then the organism divides into two equivalent organisms (**f**). The *scale bar* represents 4 μm. Reproduced from Keim et al. 2004b with permission from Blackwell

volume, not the cell number (Figs. 9a and b) (Keim et al. 2004b). This is consistent with the fact that small MMPs have smaller cells and large MMPs have larger cells (Lins and Farina 1999). To proceed in the cell cycle, all cells in an organism would divide synchronously but would remain together, resulting in a spherical MMP containing twice the cell number but approximately the same volume (Fig. 9c). The organism would become elliptical (Fig. 9d), and then eight-shaped, as two attached MMPs (Fig. 9e). The constriction between the two daughter MMPs occurs together with a slight torsion between the two halves (Fig. 9e). This torsion solves the topological problem of separating the two halves while maintaining the cell arrangement and the internal compartment. Finally, the eight-shaped MMPs would divide into two equivalent MMPs, returning to the beginning of the cycle (Fig. 9f). The whole cycle seems to last several hours, which makes impossible to follow a single organism over all stages without culturing it. The growth of the constriction (F. Abreu and U. Lins, unpublished observations) and the division of the organism into two equivalent organisms (Keim et al. 2004b; Winklhofer et al. 2005) were documented by light microscopy, as well as the presence of septa in several cells of the same MMP by TEM (Keim et al. 2004b). The fact that the magnetic moment is optimized in the whole organism can be explained by the life cycle described above, which accounts for the epigenetic inheritance of the magnetic polarity of the cells and of the whole organism (Winklhofer et al. 2005)

Cell division septa seem to occur concomitantly in all cells of a MMP. The septa always begin at the outer surface and occur radially in relation to

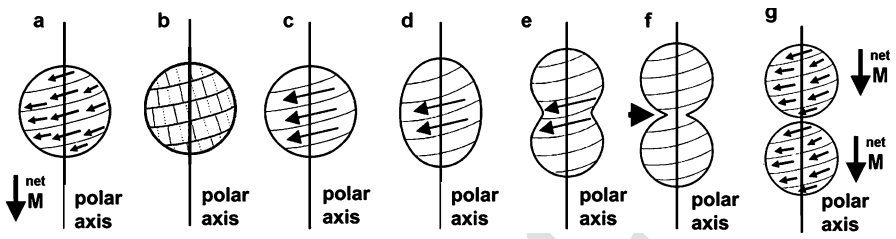

Fig. 10 Schematic drawings of magnetotactic multicelular organisms. **a** Possible distribution of the magnetic moment in a spherical organism (only the surface facing the observer is represented). The cells are arranged in a spiral, and the magnetic moment of each cell is at a fixed angle to the spiral (an example is given by the *small arrows*). The net magnetic moment of the organism is aligned to the polar axis (*large arrow*). **b** The cell division invaginations would be aligned to planes perpendicular to the laps of the spiral (*dashed lines*). **c**–**d** Cell movements during organism division. **c** The cells in neighboring laps of the spiral slide in relation to each other in the direction illustrated by the *arrows*, making the organism elongate in the direction of the polar axis. **d** After elongation, only the cells at the middle of the organism continue the movements (*arrows*), leading to a constriction. **e** Only a few cells at the middle continue the movement, until two spherical bodies are formed, linked by a single cell. **f** Now, the terminal cells separate from each other, generating two equivalent organisms similar to the parental one. **g** This process is able to generate two equal organisms with the same general cell arrangement and direction of magnetic moment as the parental one

the MMP. This special septa disposition maintains the general cell organization, i.e., all cells arranged around the internal compartment and in contact with the outer environment (Keim et al. 2004b). Furthermore, the magnetosomes, which are found in the cytoplasm mainly near the MMP outer surface (Keim et al. 2004a), and the flagella, only found in the outer surface of MMPs (Rodgers et al. 1990a), can be equally distributed between the daughter cells (Keim et al. 2004b).

The organization of cells in the MMPs in a helical pattern (Lins de Barros et al. 1990a; Keim et al. 2004b), and the torsion observed in the "eight-shaped" stage of the life cycle suggest a series of cell movements to divide one MMP into two new MMPs. The cells would be arranged as a string coiled around the internal compartment. The cells would bind less strongly to cells of other laps of the string, and the different laps would slide in relation to each other during the elongation of the organism, leading to the elliptical and eight-shaped stages, as illustrated in Fig. 10.

6
A Proposed Mathematical Model for Division and Magnetization of MMPs

To obtain a unique interpretation for all magnetic properties and movement characteristics compatible with the life cycle, an appropriate topological

model can be proposed. This model is based in an appropriate parametrized family of curves (Cassini's oval). These curves have a very simple analytical expression in polar coordinates:

$$\mathbf{r}^4 + \mathbf{a}^4 - 2\mathbf{a}^2\mathbf{r}^2 \cos(2\boldsymbol{\theta}) = \mathbf{b}^4 \quad (1)$$

where **r** and $\boldsymbol{\theta}$ are the usual polar coordinates and **a** and **b** parameters. The parameter **b** is associated with the size of the curve, and **a** is associated with the shape of the curve. When **a** = 0 the Cassini's oval is reduced to a circumference of radius **b** (i.e., **r** = **b**). When **a** = **b**, the Cassini's oval is the leminiscate of Bernoulli. Using the Cassini's oval as generator of a revolution surface and making the convolution with a cylindrical helix, a three-dimensional spiral is obtained, which changes form as a function of the parameters **a** and **b**.

The life cycle stages of MMPs observed in SEM images (Fig. 9) can be emulated by two steps in the mathematical model:

1. Growing **b**, with **a** = 0, the radius of the sphere grows; e.g., variation of parameter **b** from 0.79 to 1, increases the volume twofold. This corresponds to the observed growing in size of each individual cell during the initial phase of the life cycle.
2. Variation of parameter **a** from 0 to 1.2, maintaining **b** constant (Fig. 11). Changing **a**, changes the revolution surface and gives rise to two spheres. The shape of the surface changes (from a sphere to a melon, when **a** is varied from 0 to 0.999; when **a** = 1 the surface has a singularity; for **a** > 1 two separate surfaces are generated).

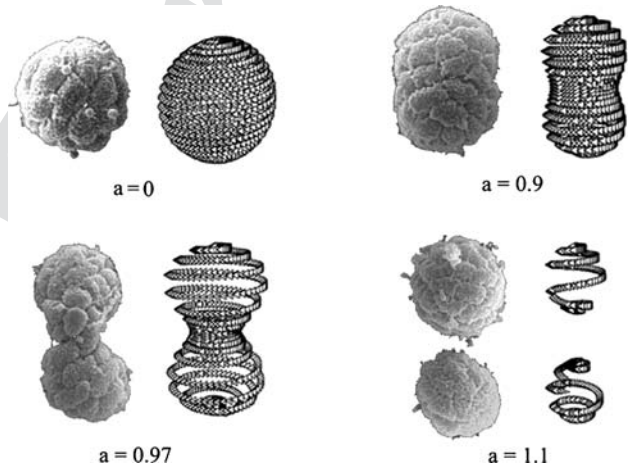

Fig. 11 Mathematical model proposed to interpret the magnetic properties and movement characteristics compatible with the observed life cycle of MMP. The Cassini's oval generated a revolution surface that was convoluted with a cylindrical helix. A three-dimensional spiral is generated, which changes form as a function of parameters **a** and **b**. In the present simulations **b** = 1

This model assumes that the cells are distributed in a spiral array in the sphere (Farina et al. 1983, 1990; Keim et al. 2004b; Lins de Barros et al. 1990; Lins and Farina, 1999), that all the cells contact the internal acellular region (Keim et al. 2004a), and that the magnetic crystals are found near the external surface of the cells (Silva et al. 2003). In addition, each cell would have a net magnetic moment nearly tangent to the sphere surface, in a direction that follows the trace of the spiral at each point, and thus inclined with respect to the symmetry axis. This distribution of magnetic crystals is a spatial distribution. When the organism is exposed to an intense magnetic field, it is possible to align individual magnetic moments and increase the total magnetization of the organism (Winklhofer et al. submitted). When the organism is exposed to a demagnetizing field, each planar array can change the magnetization polarity, and the total magnetic moment of the whole organism may be zero (Rodgers et al. 1990a,b). This division of one sphere into two equal spheres maintains the center region always isolated from the external environment.

Because of the helical symmetry of the spatial distribution of cell magnetic moments, the total magnetic moment of the organism (the vectorial sum of magnetic moments of all cells) is nearly parallel to the symmetry axis. Flagella would obey the same distribution (see Sect. 7.1 below).

7 Motility of MMPs

The study of movement of MMPs in the presence of a known applied magnetic field gives important clues for understanding magnetic properties, flagellar action, and coordination between cells of the organisms. Samples (sediments and water) from Araruama Lagoon were stored in a rectangular glass aquarium of 14 x 28 x 12 (depth) cm in the laboratory.

A pair of Helmholtz coils coupled to a DC source was adapted to the microscope stage. With this device, it was possible to generate a maximum homogeneous magnetic field of the order of 15 Gauss parallel to the glass slide (for a short period of time it was possible to obtain fields of approximately 50 Gauss). A special coil was used to obtain magnetic fields up to 10 Gauss perpendicular to the glass cover slip. The field generated was constant in the observation region, which means that no net magnetic force acts on the organism.

The movement of microorganisms in water is an example of physics at a very low Reynolds number (Purcell 1977). There is no inertial effect and, in a simple way, it is possible to treat the problem considering force as being proportional to the velocity. Acceleration does not appear in the equations. In this extreme regime, the resultant force that acts in the organism is parallel to its trajectory. MMPs present a complex behavior with respect to the movement. We propose four types of motility for them in the presence of

a homogeneous magnetic field: free motion, rotation, escape motility (or ping-pong), and walking.

7.1 Free Motion

When a uniform magnetic field is applied, MMPs swim in either straight or helical trajectories (Keim et al. 2004a). Most MMPs swim in a very elongated helical trajectory when compared to the unicellular MB (H. Lins de Barros, unpublished observation). When no obstacle is present, MMPs from Araruama Lagoon swim at 90 ± 20 μm/s. However, velocity can change from one sample to the other, or after a certain period of observation time under the light microscope. For example, after about 20 min, the velocity of the same population decreased to 64 ± 23 μm/s (Almeida et al. 2005).

Observations made with the perpendicular applied field (parallel to the optical axis of the microscope) shows that MMPs swim in a helical trajectory with the symmetry axis aligned to the magnetic field, with a typical radius of the order of some tens of microns, and pitch varying from one sample to the other. Both the helix and the MMP body rotate in the same sense of the trajectory, i.e., clockwise (in accordance to Simmons et al. 2004). Moreover, it was observed that, in one pitch, the body rotates 2π (Fig. 12a). This rotation cannot be explained by assuming that flagella form a single bundle (in this case, by the application of Newton's third law, the sense of rotation of a body would be opposite to the sense of rotation of the helix of the trajectory). It is possible

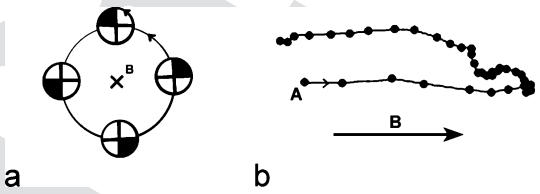

Fig. 12 Trajectories of MMPs. **a** Schedule of the trajectory (*large circle*) and rotation of the MMP (*small circles*) during motion in the direction perpendicular to the image plane (approaching the observer), based on microscopy observation through the vertical axis. The magnetic field *B* points inwards (opposite to the displacement of the south-seeking magnetotactic organism). Note that both the trajectory and the organism's body have the same sense of rotation and the same pitch. **b** Escape motility (or ping-pong) observed near the edge of a drop (*left side* in the figure). The trajectory of one MMP was projected in the xy plane. The image represents an organism swimming approximately in the horizontal plane. Note that the movement in the backward direction (to the *right*, beginning in *A*) is decelerated while the movement in the forward direction is accelerated. The distance between two *dots* in the figure represents the distance swam by the organism in approximately 1/12 s. Applied field $B = 2$ Gauss. The length of the backward movement is approximately 50 μm

that the short flagella observed act at a tangent to or obliquely to the surface of the organism, producing a resultant force that presses around the symmetry axis, making the sense of rotation of the body organism the same as that of the helical trajectory (Fig. 12a). All MMPs observed had the same sense of rotation of the body and the trajectory (H. Lins de Barros, unpublished observations).

7.2 Rotation

MMPs magnetically concentrated at the edge of a drop of water rotate around an axis that passes through the center of the organisms. Observation using a coil to produce a perpendicular magnetic field shows that when the organism is bound by an obstacle (like a small grain of sand or a fragment of sediment), the same rotation pattern is observed. Thus the edge of the drop seems to act as a mechanical stimulus to rotation. In some cases, the rotation of the body is opposite to the rotation performed during free motion (H. Lins de Barros, unpublished observation). This could be associated with a reaction of the organism to the mechanical stimulus.

7.3 Escape Motility

Perhaps the most peculiar behavior of MMPs with respect to motility is the so called "ping-pong", excursion (Greenberg et al. 2005; Keim et al. 2004a; Lins and Farina 1999; Lins de Barros et al. 1990a; Rodgers et al. 1990a; Simmons et al. 2004) or escape motility (a denomination considered in this work to be more appropriate for describing this type of motion). This movement consists of a backward movement (south-seeking in the northern hemisphere and north-seeking in the southern hemisphere) for some tens or hundreds of micrometers, followed by a forward movement (Fig. 12b) (Greenberg et al. 2005; Keim et al. 2004a; Lins de Barros et al. 1990a; Lins and Farina, 1999, 2001; Rodgers et al. 1990a). The backward movement decelerates continuously with time, whereas the forward movement that follows shows uniform acceleration (Fig. 12b) (Greenberg et al. 2005).

Observation in slow motion video shows that MMPs maintain the same orientation with respect to the magnetic field lines when they invert the sense of rotation of the body, which suggests that a change in the rotation of flagella is responsible for the escape motility (H. Lins de Barros, unpublished observation). Thus, the forward movement is clockwise, and the backward movement is counterclockwise, as also observed by Simmons et al. (2004). During the escape motility, the MMPs achieve velocities of $170 \pm 25\ \mu m/s$. The deceleration observed during the backward movement (Greenberg et al. 2005) can be caused by a gradual reduction in the flagellar rotation or in the

number of active flagella, producing an uniform decrease in the propelling force. Then, the flagella rotate in the usual direction, and the organism swims as in free motion. Thus, the observed movement is caused by the coordinated action of flagella, meaning that the velocity varies during this movement as a consequence of the change in flagellar action.

Because the probability for an MMP to begin a backward excursion increases with the magnetic field strength, it was proposed that they present a magnetoreception mechanism (in magnetic fields larger than the Earth's) (Greenberg et al. 2005).

7.4 Walking

At magnetic fields of the order of magnitude of the Earth's magnetic field, MMPs swim at constant velocity in a looping motion near the water–air interface (Greenberg et al. 2005). The use of an applied magnetic field perpendicular to the glass slide allowed us to analyze the trajectories during these loops. It was observed that when MMPs reach the air–water interface on the top of the drop, they walk freely in a complex trajectory, maintaining, however, the same sense of body rotation. In this situation, the organism did not present escape motility (H. Lins de Barros, unpublished observation).

8 Magnetic Properties of MMPs

MMPs collected in Araruama Lagoon are south-seeking magnetotactic organisms. The process of magnetic concentration in the laboratory (described in detail by Lins et al. 2003) can artificially introduce a bias in the observations. However, using the same method but changing the polarity of magnets, a very small number of MMPs is observed with a magnetic response that corresponds to north-seeking organisms. Observations made with very rich populations, collected as described above, show that a very small number of MMPs with opposite polarity are present in the sample.

The most striking characteristic of magnetotactic microorganisms is their capacity to align to the lines of a magnetic field. Magnetotaxis can be explained by using the direct application of dipole-magnetic field interaction theory. The simplest method for estimating the total magnetic moment of a magnetotatic microorganism is the "U-turn" method (Lins de Barros et al. 1990b). This method is based on the assumption that, statistically, a population of magnetotactic organisms can be treated as a population of non-interacting dipoles, and the mean orientation of the dipoles is given by the theory of paramagnetism of Langevin (Frankel and Blakemore 1980). The U-turn method gives the relation between the total magnetic moment of the

organism, m, and the diameter of the trajectory (U-turn), L, when the applied field is suddenly reversed. The method also gives the time, T_{u}, that the organism needed to perform the U-turn. Comparison between T_{u} and the measured time, T_{exp}, is an important way to guarantee the precision of the estimate of m. The trajectory diameter, **L**, and the time of the U-turn, T_u, are given by the following equations (assuming a spherical body with radius R translating with migration velocity v, in a medium with viscosity η in a external magnetic field B at an absolute temperature T):

$$m = 8\pi^2 \eta R^3 v/LB \; T_{\mathrm{u}} = (8\pi\eta R^3/\mathrm{m}B) ln(2\mathrm{m}B/\mathrm{k}T) \tag{2}$$

where k is the Boltzmann constant. The total magnetic moment, m, depends on R^3.

Simultaneous measurements of v, R, B, L and T_{exp} can be made using a video recorder and analyzing the images frame by frame. Considering only values of m that give T_{u} with an error of less than 10% when compared with T_{exp}, it is observed that the total magnetic moment of MMPs has a distribution with two peaks, one centered at $(1.0 \pm 0.3) \times 10^{-10}$ emu, and the other at $(1.8 \pm 0.3) \times 10^{-10}$ emu.

8.1 Magnetization, Demagnetization and Remagnetization

Experiments on the alignment of the MMPs from Araruama Lagoon to a laboratory magnetic field of the order of 10 Gauss and submitting the organism to an applied pulse (of the order of 1 millisecond) of circa 1000 Gauss showed that the net magnetization of the organism grows only about 20% with respect to the natural magnetization. This indicates that the crystal magnetic distribution is optimized in the MMPs (Winklhofer et al. 2005).

When MMPs were exposed to a 60 Hz AC magnetic field, they could be remagnetized (many originally north-seeking MMPs could migrate as south-seeking microorganisms), indicating that the intact organism has an axis of motility (Rodgers et al. 1990a,b), similar to unicellular magnetotactic bacteria (Blakemore et al. 1980). Unlike the cells of *Magnetospirillum magnetotacticum*, a cultivated magnetite producer, the MMP hysteresis loops were not square, indicating that they could be demagnetized (Penninga et al. 1995). Accordingly, after exposure to a 60 Hz AC magnetic field some organisms were demagnetized and subsequently failed to respond to changes in the magnetic field, and swam in random directions (Rodgers et al. 1990a).

Demagnetization experiments were made in magnetically concentrated samples from Araruama Lagoon. A commercial tape recorder demagnetizer (60 Hz, 600 Gauss) was used. The samples were exposed for a few seconds and observed in the microscope. After the demagnetization process, the MMPs presented no response to an applied magnetic field. This could be a consequence of the complex spatial distribution of magnetic crystals that produces

a multipolar field. The interaction between crystal arrays of different cells of the same organism is insufficient to change the polarity of the arrays. However, after demagnetization, each cell can present a different polarization, giving a net magnetic moment of the whole MMP near zero. When demagnetized samples were exposed to an intense field produced by a magnet (Sm Co industrial magnet), remagnetization of the organisms was observed. This remagnetization produced predominantly organisms of the same original polarity (H. Lins de Barros, unpublished observation).

9 Are MMPs Really Multicellular Organisms?

The answer to the above question depends on the concept used to define a multicellular organism. Traditional concepts based on animal and plant studies include the presence of different cell types and a characteristic cell organization in tissues and/or organs (Gilbert, 2003). "Mid-way" concepts require specific organism shape and cell organization and lack of cell autonomy and competition in order to consider an organism multicellular (Carlile 1980). Current concepts arose as a consequence of new discoveries that challenged the conventional way of thinking. What once was based mainly on morphology now incorporates cell-to-cell signaling and behavior. For example, Shapiro (1998) and Kaiser (2001) proposed that multicellular organisms have many cells in close contact that coordinate growth, movements, and biochemical activities.

MMPs do not seem to have different cell types, and thus do not fulfill the traditional requirements for a multicellular organism. On the other hand, with the present knowledge, MMPs perfectly fit the mid-way concept proposed by Carlile (1980) and the modern concepts of Shapiro (1998) and Kaiser (2001): their cells are closely apposed and organized in a characteristic way, are not autonomous, seem not to compete with each other, and coordinate cell division and movements. Furthermore, the MMPs were never observed as single cells (Farina et al. 1990, Lins de Barros et al. 1990; Lins and Farina 1999; Mann et al. 1990; Rodgers et al. 1990).

10 Conclusions

In this chapter we have discussed several aspects of the biology and biophysics of the magnetotactic multicellular organisms. It was shown that after the first description of MMPs (Farina et al. 1983), it took 7 years for the appearance of papers showing the presence of a new biomineralized magnetic material inside their cytoplasm: the iron sulfide magnetic crystals, different

from the iron oxide magnetite known at that time in magnetosomes (Farina et al. 1990; Mann et al. 1990). Eight more years were needed to build a consistent model to explain the reaction sequence related to the production of the magnetic iron sulfides in MMPs (Pósfai et al, 1998a,b). Only recently, has the morphology of MMPs been studied in detail (Keim et al. 2004a) and a cell cycle proposed (Keim et al. 2004b). A detailed study on the motility of the organisms in applied magnetic fields was also performed (Greenberg et al. 2005).

Curiously, only one paper exists on the phylogenetic affiliation of the MMP (DeLong et al. 1993). From this comprehensive review of the literature on MMPs, we now see that it is time for the contributions that can be achieved using a molecular biology approach. The first deep insights into the structure of MMPs were obtained from high resolution electron microscopy studies of the iron mineral inclusions, which meant solving questions directly related to biomineralization. Nowadays, fundamental questions on the biology of the MMPs arise. These are mainly related to multicellularity in prokaryotes, cell division and magnetoreception, and information transduction. There are also new biomineralization questions related to MMPs after the finding that magnetic crystals inside MMPs from the same environment can be composed of iron sulfides, iron sulfides together with iron oxides, or only iron oxides.

We have presented in this chapter a unified hypothesis linking cell organization, proliferation, magnetism, and motility of MMPs, which is based on experiments and direct observation of the microorganism. Further work is necessary to strengthen or correct some points, but all knowledge accumulated up to now is in accordance with our hypothesis. We believe that further work on 16S rDNA phylogeny, ecology, behavior, magnetic properties, and ultrastructure will increase the breadth of a unified view of these interesting microorganisms.

Acknowledgements UL acknowledges partial support from CNPq (Pronex). MF acknowledges CNPq and FAPERJ Brazilian Agencies. We are indebted to the staff of "Laboratório de Ultraestrutura Celular Hertha Meyer" at the Biophysical Institute, Federal University of Rio de Janeiro, for the electron microscopy facilities.

References

Almeida FP, Farina M, Keim, CN (2005) Angular dispersion of magnetotactic multicellular organisms trajectories in an applied magnetic field. Braz J Morphol Sci (suppl. 2005), p 207

Bazylinski DA, Frankel RB (2004) Magnetosome formation in prokaryotes. Nature Rev Microbiol 2:217–230

Bazylinski DA, Frankel RB, Garratt-Reed AJ, Mann S (1990) Biomineralization of iron sulfides in magnetotactic bacteria from sulfidic environments. In: Frankel RB, Blakemore RP (eds) Iron biominerals. Plenum, New York, pp 239–255

Bazylinski DA, Garratt-Reed AJ, Abedi A, Frankel R (1993) Copper association with iron sulfide magnetosomes in a magnetotactic bacterium. Arch Microbiol 160:35–42

Bazylinski DA, Frankel RB, Heywood BR, Mann S, King JW, Donaghay PL, Hanson AK (1995) Controlled biomineralization of magnetite (Fe_3O_4) and greigite (Fe_3S_4) in a magnetotactic bacterium. Appl Environ Microbiol 61:3232–3239

Blakemore RP (1975) Magnetotactic bacteria. Science 190:377–379

Blakemore RP (1982) Magnetotactic bacteria. Annu Rev Microbiol 36:217–238

Blakemore RP, Frankel RB, Kalmijn AJ (1980) South-seeking magnetotactic bacteria in the Southern Hemisphere. Nature 286:384–385

Buseck PR, Pósfai M, Dunin-Borkowski RE, Weyland M (2003) Iron oxide and sulfide nanocrystals as biomarkers. Microsc Microanal 9(suppl 2):242–243

Carlile MJ (1980) From prokaryote to eukaryote: gains and losses. In: Gooday GW, Lloyd D, Trinci APJ (eds) The eukaryotic microbial cell. Cambridge University Press, pp 1–38

DeLong EF, Frankel RB, Bazylinski DA (1993) Multiple evolutionary origins of magnetotaxis in bacteria. Science 259:803–806

Devouard B, Posfai M, Hua X, Bazylinski DA, Frankel RB, Buseck PR (1998) Magnetite from magnetotactic bacteria: Size distributions and twinning. Amer Mineral 83:1387–1399

Enrich-Prast A, Bozelli RL, Esteves FA, Meirelles FP (2003) Lagoas Costeiras do Parque Nacional da Restinga de Jurubatiba: descrição de suas variáveis limnológicas. In: Rocha CFD, Esteves FA, Scarano FR (eds) Ecologia, história natural e conservação do Parque Nacional da Restinga de Jurubatiba

Farina M, Lins de Barros HGP, Esquivel DMS, Danon J (1983) Ultrastructure of a magnetotactic microorganism. Biol Cell 48:85–88

Farina M, Esquivel DMS, Lins de Barros HGP (1990) Magnetic iron-sulphur crystals from a magnetotactic microorganism. Nature 343:256–258

Flies CB, Peplies J, Schüler D (2005) Combined approach for characterization of uncultivated magnetotactic bacteria from various aquatic environments. Appl Environ Microbiol 71:2723–2731

Frankel RB, Blakemore RP, Wolfe RS (1979) Magnetite in freshwater magnetotactic bacteria. Science 203:1355–1356

Frankel, RB, Blakemore, RP (1980) Navigational compass in magnetic bacteria. J Magnetism Magnetic Mater 15–18(Part 3):1562–1564.

Frankel RB, Bazylinski DA, Johnson MS, Taylor BL (1997) Magneto-aerotaxis in marine coccoid bacteria. Biophys J 73:994–1000

Gilbert SF (2003) Developmental biology, 7th edn. Sinauer, Sunderland, MA, USA

Greenberg M, Canter K, Mahler I, Tornheim A (2005) Observation of magnetoreceptive behavior in a multicellular magnetotactic prokaryote in higher than geomagnetic fields. Biophys J 88:1496–1499

Kaiser D (2001) Building a multicellular organism. Annu Rev Genet 35:103–123

Keim CN, Lins U, Farina M (2003) Iron oxide and iron sulphide crystals in magnetotactic multicellular aggregates. XIX Congress of the Brazilian Society for Microscopy and Microanalysis. Acta Microsc. 12(suppl B):3–4

Keim CN, Abreu F, Lins U, Lins de Barros HGP, Farina M (2004a) Cell organization and ultrastructure of a magnetotactic multicellular organism. J Struct Biol 145:254–262

Keim CN, Martins JL, Abreu F, Rosado A, Lins de Barros HGP, Borojevic R, Lins U, Farina M (2004b) Multicellular life cycle of magnetotactic prokaryotes. FEMS Microbiol Lett 240:203–208

Kirschvink JL (1980) South-seeking magnetic bacteria. J Exp Biol 86:345–347

Kjerfve B, Schettini CAF, Knoppers B, Lessa G, Ferreira HO (1996) Hydrology and salt balance in a large, hypersaline coastal lagoon: Lagoa de Araruama, Brazil. Estuar Coast Shelf Sci 42:701–725

Lins de Barros HGP, Esquivel DMS, Farina M (1990a) Biomineralization of a new material by a magnetotactic microorganism. In: Frankel RB, Blakemore RP (eds) Iron biominerals. Plenum, New York, pp 257–268

Lins de Barros HGP, Esquivel DMS, Farina M (1990b) Magnetotaxis. Sci Progress 74:347–359

Lins U, Farina M (1999) Organization of cells in magnetotactic muticellular aggregates. Microbiol Res 154:9–13

Lins U, Farina M (2001) Amorphous mineral phases in magnetotactic multicellular aggregates. Arch Microbiol 176:323–328

Lins U, Farina M, Lins de Barros HGP (1992) Contribution of electron spectroscopic imaging to the observation of magnetic bacteria magnetosomes. Microsc Eletr Biol Cel 16:151–162

Lins U, Freitas F, Keim CN, Farina M (2000) Electron spectroscopic imaging of magnetotactic bacteria: magnetosome morphology and diversity. Microsc Microanal 6:463–470

Lins U, Freitas F, Keim CN, Lins de Barros H, Esquivel DMS, Farina M (2003) Simple homemade apparatus for harvesting uncultured magnetotactic microorganisms. Braz J Microbiol 34:111–116

Lumsden CJ (1984) Dual inheritance in haploid organisms: a model of magnetotactic bacteria. J Theor Biol 111:1–16

Mann S, Sparks NHC, Frankel RB, Bazylinski DA, Jannasch HW (1990) Biomineralization of ferrimagentic greigite (Fe_3S_4) and iron pyrite (FeS) in a magnetotactic bacterium. Nature 343:258–261

Penninga I, Waard H, Moskowitz BM, Bazylinski DA, Frankel RB (1995) Remanence measurements on individual magnetotactic bacteria using a pulsed-field magnetic field. J Mag Mag Mater 149:279–286

Pósfai M, Buseck PR, Bazylinski DA, Frankel RB (1998a) Reaction sequence of iron sulfide minerals in bacteria and their use as biomarkers. Science 280:880–883

Pósfai M, Buseck PR, Bazylinski DA, Frankel RB (1998b) Iron sulfides from magnetotactic bacteria: structure, composition, and phase transitions. Am Mineral 83:1469–1481

Pósfai M, Cziner K, Márton E, Márton P, Buseck PR, Frankel RB, Bazylinski DA (2001) Crystal-size distributions and possible biogenic origin of Fe sulfides. Eur J Mineral 13:691–703

Purcell EM (1977) Life at low Reynolds number. Am J Physics 45:3–11

Rodgers FG, Blakemore RP, Blakemore NA, Frankel RB, Bazylinski DA, Maratea D, Rodgers C (1990a). Intercellular structure in a many-celled magnetotactic prokaryote. Arch Microbiol 154:18–22

Rodgers FG, Blakemore RP, Blakemore NA, Frankel RB, Bazylinski DA, Maratea D, Rodgers C (1990b) Intercellular junctions, motility and magnetosome structure in a multicellular magnetotactic prokaryote. In: Frankel RB, Blakemore RP (eds) Iron biominerals. Plenum, New York, pp 231–237

Shapiro JA (1998) Thinking about bacterial populations as multicellular organisms. Annu Rev Microbiol 52:81–104

Silva KT, Keim CN, Abreu F, Martins JL, Rosado AS, Farina M, Lins U (2003) Spatial relationships of cells within magnetotactic multicellular aggregates. Acta Microsc 12 (suppl. B):367–368

Simmons SL, Sievert SM, Frankel RB, Bazylinski DA, Edwards KJ (2004) Spatiotemporal distribution of marine magnetotactic bacteria in a seasonally stratified coastal salt pond. Appl Environ Microbiol 70:6230–6239

Simmons SL, Bazylinski DA, Edwards KJ (2006). South-seeking magnetotactic bacteria in the northern hemisphere. Science 311:371–374

Spring S, Lins U, Amann R, Schleifer K-H, Ferreira LCS, Esquivel DMS, Farina M (1998) Phylogenetic affiliation and ultrastructure of uncultured magnetotactic bacteria with unusually large magnetosomes. Arch Microbiol 169:136–147

Williams R (1979) The geometrical foundation of natural structure. Dover, New York

Winklhofer M, Abraçado LG, Davila AF, Keim CN, Petersen N and Lins de Barros HGP (2005) Magnetic properties of a multicellular magnetotactic prokaryote, RIN 05 Animal Navigation Conference, London